Article

Effective electrical conductivity performance of a 25% antimonial lead alloy-air battery cell made with ESR open cell foams as electrode

Amel Hind Hassein-Bey [1], Abd-Elmouneïm Belhadj [1], Selma Toumi [2], Hichem Tahraoui [1,3], Mohammed Kebir [4], Abdeltif Amrane [5*], Derradji Chebli [3], Abdallah Bouguettoucha [3], Jie Zhang [6], and Lotfi Mouni [7]

[1] Laboratory of Biomaterials and Transport Phenomena (LBMTP), University Yahia Fares, Médéa, 26 000, Algeria
[2] Faculty of Sciences, University of Medea, Nouveau pôle Urbain, Medea University, 26000 Medea, Algeria
[3] Laboratoire de Génie des Procédés Chimiques, Department of process engineering, University of Ferhat Abbas, Setif, Algeria
[4] Research Unit on Analysis and Technological Development in Environment (URADTE-CRAPC), BP 384, Bou-Ismail Tipaza, Algeria.
[5] Univ Rennes, Ecole Nationale Supérieure de Chimie de Rennes, CNRS, ISCR – UMR6226, F-35000 Rennes, France.
[6] School of Engineering, Merz Court, Newcastle University, Newcastle upon Tyne NE1 7RU.
[7] Laboratory of Management and Valorization of Natural Resources and Quality Assurance, SNVST Faculty, Akli Mohand Oulhadj University, Bouira 10000, Algeria.

*Correspondence: E-mail: abdeltif.amrane@univ-rennes1.fr;

Abstract: The global context of research for new sustainable energy storage technologies makes it a very active sector with significant scientific and economic challenges. Indeed, due to the irregular development of renewable energies and the shutdown of traditional power facilities, it is difficult to maintain a stable balance in terms of supply and demand: energy storage can help in particular for substantial changes in the latter. Metal air batteries have a higher energy density and are safer than other available energy storage devices. Based on the existing and proven lead-acid battery technology, this paper proposed an open cell foam manufactured by the Excess Salt Replication process for use as an anode for lead-air battery cells with sulphuric acid as the electrolyte. This will save lead and reduce the battery weight. A 25% antimonial lead alloy was used to produce open cell foams with a cell diameter between 2 mm and 5 mm for the antimonial lead-air battery. Preliminary results of the effective electrical conductivity of primary battery cells, measured experimentally, showed that all antimonial lead foam-air battery cells performed better than that made from the same dense non porous antimonial lead alloy. This is generally due to their important specific surface area where oxidation-reduction reactions took place. A correlation between the effective electrical conductivity and the cell diameter has been established and the highest conductivity was obtained with a cell diameter of 5mm. The feasibility of such an electrical system has been demonstrated.

Keywords: Metal-air battery cell; electrode materials; open cell foam; replication process; effective conductivity

1. Introduction

Nowadays, all studies in the field of energy storage are trying to improve the electrical performance of batteries while making them lighter [1-7]. Despite this, lead acid batteries are still the most widely used, for example in the automotive industry, as in 2010 they accounted for 99% by weight of batteries used in this field. The main advantages of this technology are its low cost at

 doi:10.20944/preprints202305.0296.v1

around 150 €/kWh [8], and its good efficiency of 75% to 80% [9]. Its simplicity and strength have made it the leader in the field of energy storage for more than one and half centuries. Many researchers are trying to overcome the drawbacks of these batteries, either by improving the electrolyte or by working on the electrode alloys [10-15], or even by the development of lightweight lead acid batteries grids [16-23] which may reduce cost, effort, and materials. Lach et al. [24] confirmed that replacement of a standard grid in a lead-acid battery with a reticulated vitreous carbon (RVC) or conductive porous carbon (CPC) leads to the reduction of battery weight and lead consumption by about 20%.

Recently metal-air batteries (MABs) have immerged and been intensively studied as promising and efficient batteries for different applications [25-29]. They are compact and light energy sources with a high energy density [28,30]. In such electrochemical systems oxygen from the air is used as a cathode along with a liquid electrolyte. This contributes to lowering the cost and weight of the MABs. Metal electrodes can be zinc, lithium, magnesium, aluminium, and other metals. This device's fundamental working concept is to electrochemically reduce O2 from the air and oxidize the metal electrode, resulting in the formation of solid metal oxides that may be recycled [31].

Different metals have been used as electrodes for MAB. Zinc-air batteries (ZAB) are the only fully developed metal-air systems currently available, and have been successfully marketed as non-rechargeable cells for several decades. Nevertheless, Pei et al. [32] stated that the lifespan and electrical rechargeability of ZAB are both limited. Even Li-air battery was considered the most promising among the other MABs, but it could not be industrialised. Akhtar et al. [33] concluded that low discharge rate, lower number of cycles, oxidation of lithium anode, discharge products at cathode, and side reactions inside the battery were the key limiting factors in the slow progress of Li-air batteries on an industrial scale. Rechargeable Na-air batteries are the subject of great interest nowadays because of their high theoretical specific energy density, lower cost, and lower charge potential compared with Li-air batteries. However, high purity O2 used as a working environment is required to achieve high –performance, which obstructs their application as a high-energy-density battery [34]. Aluminium–air batteries using alkaline electrolyte have good battery performance, especially under high discharge current. However, alkaline electrolytes and aluminium electrodes tend to be highly corrosive, and the main problem restricting a feasible usage of Al–air batteries is the low coulomb efficiency resulting from the self-corrosion of the electrode. To overcome this problem, aluminium alloys have been chosen as the electrode material [35]. Zhao et al. [36] reported that adding vanadate or phosphate as a corrosion inhibitor to the NaCl electrolyte significantly improved the performance of Mg-air batteries, and phosphate showed a stronger inhibiting effect than vanadate. The Sn-air batteries are another type of MAB which operate at room temperature with an electrolyte of methane sulfonic acid and polyacrylamide gel [37]. Most recently, Milusheva et al. [30] showed the possibility of utilization of the lead-air electrochemical system as a power source. This system consisted of a standard lead electrode and H2SO4 electrolyte, used in the lead-acid battery and a gas diffusion electrode which was sufficiently stable in the sulphuric acid electrolyte. They concluded that the energy values obtained at laboratory conditions provided a good perspective for a practical application of the lead-air system for energy storage and in the automobile industry.

The most common customer complaints about power supply systems have always revolved around two factors: battery life and weight, especially for vehicles. Because it takes less energy to accelerate a lighter object than a heavier one, so lightweight batteries offer great potential for increasing vehicle efficiency.

It is believed that the porosity of foams provides a higher specific surface area where redox reactions take place, and improves electrical conductivity [38] for more lightweight batteries in future. The objective of this experimental work is mainly on the study of usage and electrical performance of a cellular materials like open cell metal foams as direct active electrode in this kind of batteries since only a few works exist on these batteries [28,39-41]. These foams were made available through a new variant of space holder replication technique developed using salt (NaCl) as a removable preform. This variant was named the "Excess Salt Replication process" (ESR process) [42]. In order to obtain samples of good quality, metals, and alloys of good castability are highly recommended, like the 25%antimonial lead alloy (25% Sb-Pb), among others, which gave samples of

 doi:10.20944/preprints202305.0296.v1

porosity between 46% and 66%. These open cell foams were made from grain of salt with diameters ranging from 2mm to 5mm. So the choice of the 25% antimonial lead alloy concentration is based on technical reasons related to the ESR process, because it is well known that at concentrations above 4% of antimony (Sb), it tends to be released from the grid into the electrolyte during operation and charging in lead-acid batteries. The released antimony is deposited on the lead foam of the negative plate [43]. This results in a reduction in hydrogen overvoltage and the local lead and antimony cells on the negative plate also cause an open circuit loss of charge. So, it is desirable to reduce the antimony content as much as possible in order to reduce open circuit losses and to make the battery cell resistant to the adverse effects of overcharging, which tends to occur with automotive batteries charged from AC sources, e.g. alternators. Nevertheless, antimony is generally added also to improve the strength and castability of the alloy, and for its high corrosion resistance [44]. The effect of Sb concentration in the antimonial lead alloy designed for the electrode of these metal foam air battery cells (MFABs) will be discussed in further research.

Scientific work on the electrochemistry of cellular materials is very scarce and only a few data on the electrical conductivity of cellular metals have been reported so far [45,46]. On the other hand, when analysing these relative electrical conductivity values from different authors, it is found that they are very different, mainly for foams produced by space holder or replication methods. Each foam has a different structure of its own since the processes of their manufacture are different [47] and therefore individual foam needs to be characterized experimentally. No one, to our knowledge, has yet studied or proposed the use of cellular materials in MABs. This study attempts to consolidate the electrochemical data on the performance of cellular materials in the field of energy storage, and especially in MABs, in order to make them lighter.

Batteries are known as either primary, i.e. not rechargeable, or secondary, meaning that they can be recharged. In this study, a primary in-laboratory reconstructed battery cells were considered.

Firstly, the effective electrical conductivity (EEC), of MFAB cells using the ESR foams as electrodes, was measured.

Secondly, the advantages of these MFAB cells were revealed through the comparison of their EEC with that of the MAB cell which electrode was non porous and was made from the same dense alloy (25% Sb-Pb). These EECs were regarded as the measurement of apparent electrolyte-foams interactions conductivity.

Then, the identification of electrodes electrochemical reactivity was necessary to confirm that they are indeed MFAB cells where ESR foam electrode electrochemical reactivity was the origin of MFAB cell electrical current. Fourier-transform infrared spectroscopy analysis of the external surface of the ESR dense electrode was done before and after cell tests.

The effect of cell diameter of ESR foam electrodes on the measured EEC was finally analysed.

2. Materials and Methods

It seemed appropriate to reconstruct a metal foam-air battery cells using different ESR foams obtained for salt grain diameters between 2mm and 5mm and to measure their cell effective electrical conductivities (EEC), K_m (μS/cm). Because the direct measurement of the electrical conductivity of a cellular material is very hard, it is assumed that the delivered electrical current from the interaction between these electrodes and the H2SO4 electrolyte, in the presence of the O2 from the air (as cathode) is representative of the electrical conductivity which is named in this case the “effective electrical conductivity”, and could be used to compare the electrical performances of cellular ESR electrodes and that made from the dense alloy of the same composition 25% Sb-Pb.

The ESR process is a simple and inexpensive technique based on the space holder replication method for elaboration of cellular materials. It consists of four steps, which are: Fused metal infiltration of the salt preform, excess salt compaction, samples cooling and salt leaching [42]. Good open cell foams with two different alloys were made with this process, namely: 25%antimonial lead alloy, which has porosity ranging from 46% to 66%; and zamak 5, which has porosity ranging from 58% to 65%. These two alloys had good castability, good fluidity, and low melting temperature below that of the salt (Tm salt=801°). In this work only 25% antimonial lead alloy was investigated.

 doi:10.20944/preprints202305.0296.v1

These researchers when investigating the ESR foam cells using Scanning Electron Microscopy, before leaching salt found the presence of lead oxide crystals formed probably during the infiltration of the salt preform by the fused metal. These crystals formed a thin film between the foam matrix and the grains of salt without affecting the cell diameter. There were two different types of crystals, elongated prismatic tubular shape and snowflakes, thin reticulated crystals.

They supposed that these lead oxides were transformed to lead carbonates after salt leaching, which was of great interest to lead batteries in general.

Hassein-Bey et al. [42] proved that the cell shapes were replicas of the NaCl grains used as space holder (after dissolution of the salt, the cells preserved the original forms and size of the grains of salt).

The EEC of H_2SO_4 is representative of that of the electrodes as it results from the spontaneously generated current from the interaction of the electrodes when placed in the sulphuric acid.

A series of electrochemical tests were carried out on reconstructed MFAB cells in the laboratory. Electrodes manufactured by the ESR process were used as anodes and the available oxygen O_2 in the air was the cathode. So, the 25 SbPb- Air cell is the MFAB designed with the equipment shown in Figure 1. This experimental stand comprising these cells, was carefully designed to explore the necessary conditions and the results of these tests:

- The ESR foam electrodes were carefully cut into regular stick shapes before the salt removal (Figure 1).
- Density of the dried foams was measured by Archimedes' principle, then porosity P was calculated. [42]
- Before and after each test, the ESR foam anode and the dense Pb were weighed.
- Stirring was carried out by the laboratory stirrer (Figure 1) for a good distribution of the species existing during the chemical reactions and for better dissolution of oxygen from the air in the electrolyte.
- The last test used the same 25% Sb-Pb dense alloy (non-porous material) as anode for comparison.
- A SELECTA CD-2005 Conductivity Meter (Figure 1) for electrolyte conductivity measurement and SELECTA pH-2005 pH Meter (Figure 1) electrochemical experimental apparatus were used simultaneously to measure the electrolyte electrical conductivity K_m and pH every 1 minute for 30 minutes, timed by Diamond digital stopwatch (Figure 1).
- The electrical current was measured once the electrodes were immersed in an agitated sulphuric acid H_2SO_4, with an average pH between 1.11 and 1.28 (Figure 1).
- The entire sample had to be immersed in the sulphuric acid electrolyte to ensure that the properties studied were representative of the totality of the sample's interactions with the electrolyte.
- The temperature of the 100 ml of sulphuric acid was also measured with a digital thermometer (Figure 1) during every manipulation (T_0 before test and T_f at the end of the test) to explore the thermal stability of the cell.

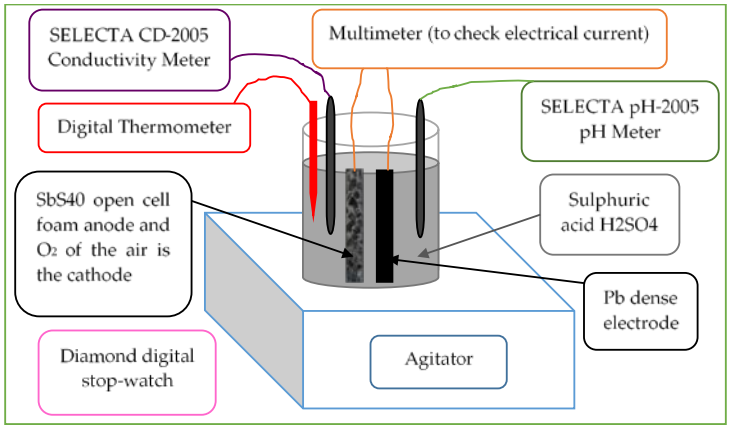

Figure 1. Experimental stand showing the test cell of the 25% SbPb- Air battery.

- Note that the battery cells were named "SbSPb X", where SbS stands for the anode foams obtained from the ESR process (see [42]); Pb was the non-porous dense lead electrode used for electrical circuit closure. A multimeter is used to check electrical current flow too and it will be shown later that this electrode does not contribute to the electrochemical reactions of the cell. X represents the value of the decimal salt grain diameter. Table 1 regroups the measured and calculated parameters of all tested samples.

Table 1. Measured and calculated parameters of all tested cells

	mF_0 (g)	mD_0 (g)	mF_f (g)	mD_f (g)	Δ mF (g)	ΔmD (g)	Dc (mm)	P (%)	T_0-T_f (°C)	K_m (µS/cm)	pH_0-pH_f
sbspb20	5,780	3,696	5,777	3,695	0,003	0,001	2,000	46	19,6-19,7	689,00	1,16-1,18
sbspb30	2,350	3,664	2,345	3,663	0,005	0,001	3,000	66	17,9-17,5	704,05	1,25-1,29
sbspb35	6,311	3,374	6,303	3,373	0,008	0,001	3,500	48	19,7-19,9	721,42	1,11-1,13
sbspb40	8,068	3,752	8,066	3,750	0,002	0,001	4,000	56	17,8-17,7	713,53	1,13-1,11
sbspb50	3,458	3,734	3,458	3,732	0,000	0,002	5,000	60	17-16,7	735,16	1,25-1,26
sbpb dense	3,695	3,869	3,698	3,871	-0,003	-0,002	-	0	17,3	678,36	1,15-1,17

The operational method for each battery cell test is summarised as:

when the two weighed electrodes are fully immersed in an agitated sulphuric acid, the measurements of EEC, T, and pH are taken every 1 minute for 30 minutes; then the dried electrodes are weighed again after cell tests; and finally the average EEC, K_m (µS/cm) was calculated.

3. Results and discussions

3.1. Interpretation of measured effective electrical conductivity results

Commonly, MFABs are electrochemical systems which rely on metal oxidation and oxygen. Oxygen from the air is used as a cathode along with a liquid electrolyte (H_2SO_4) and the metal is the anode.

The curves in Figure 2 and Figure 3 show the individual electrochemical behaviour of each ESR foam.

The effective electrical conductivity (EEC) of all cells shows a decreasing trend with time.

The conductivity of an electrolyte depends on the amount of free water it contains [48,49], which explains the decrease in conductivity during all tests due to the spontaneous activity of water (consumption of H+ ions). Majima et al. [48], when studying the electrical conductivity of an acid sulphate solution, found that the addition of metal sulphates to an aqueous sulphuric acid solution causes a decrease in electrical conductivity, and this phenomenon is attributed to a decrease in the activity of water, which reflects a decrease in the amount of free water; and on the other hand, any increase in the concentration of H+ ions leads to an increase of electrical conductivity. As the cell discharges, hydrogen ions are being removed so the concentration of hydrogen ions in the electrolyte is decreasing. The pH is therefore increasing like in lead acid batteries [42].

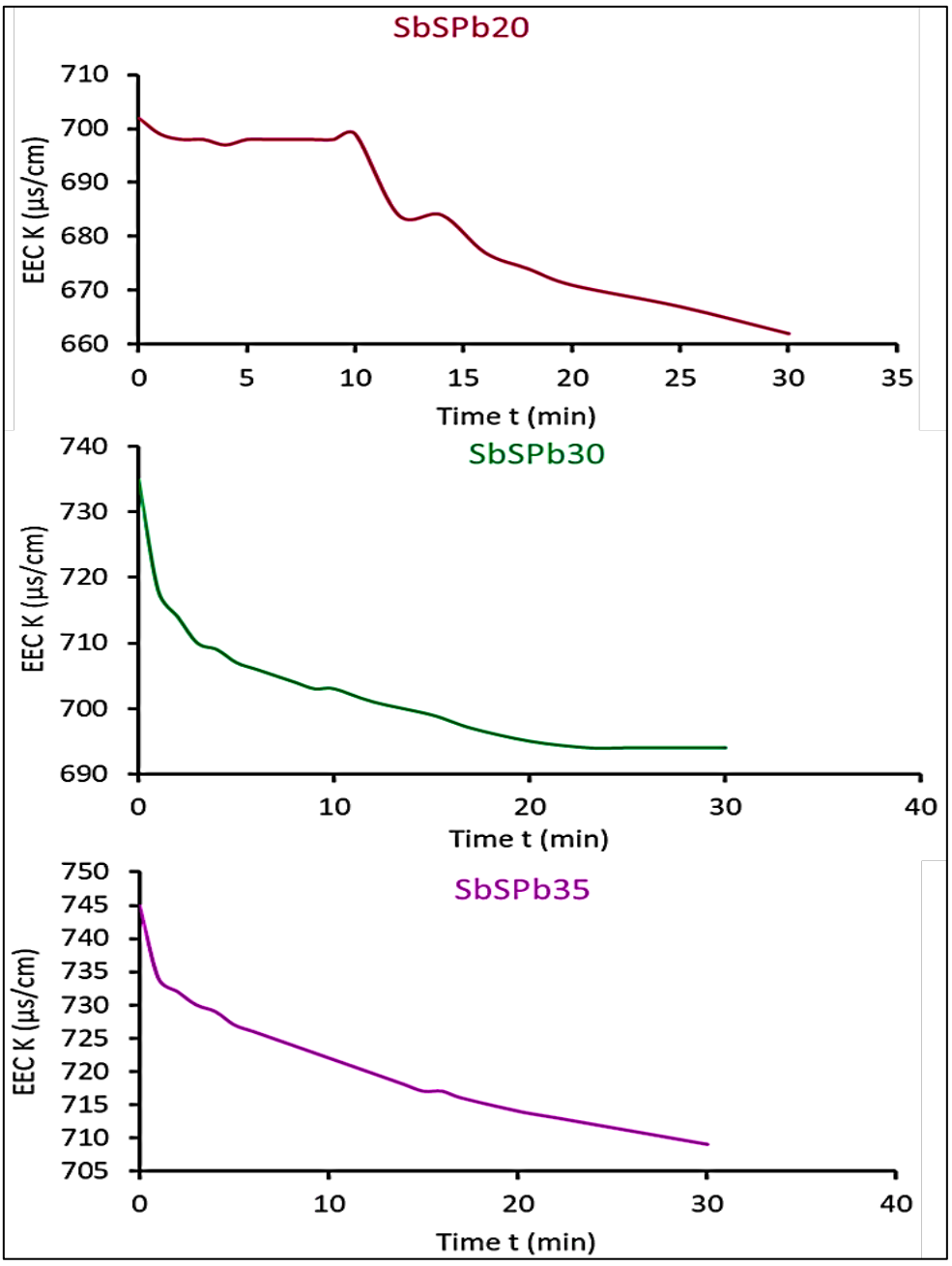

Figure 2. Curve representing the electrochemical behaviour of SbSPb20, SbSPb30 and SbSPb35 cells by measuring the effective electrical conductivity as a function of time.

Furthermore, there is a resemblance between the curve of SbSPb20 and that of dense SbPb which give a graduated decrease, however completely different from the others which are rather soft namely: SbSPb30, SbSPb35, SbSPb40, SbSPb50.

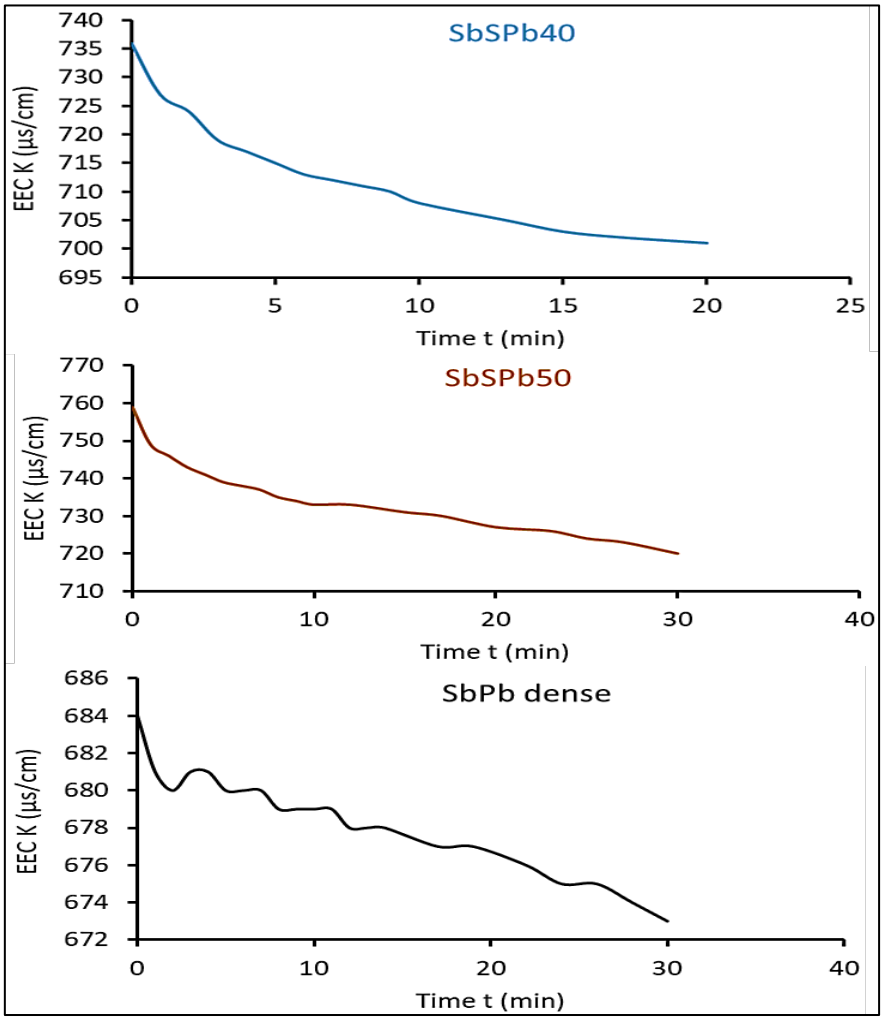

Figure 3. Curve representing the electrochemical behaviour of SbSPb40, SbSPb50 and SbPb dense cells by measuring the effective electrical conductivity as a function of time.

Table 1 displays a no relevant changes in temperatures in general for all testedcells. This means that MFAB cells are thermally stable.

3.3. Advantages of ESR foams and electrodes reactions

In order to compare MFAB cells performances to that of the non-porous dense alloy; all curves had been regrouped in one graph represented on Figure 4. It is shown that the electrical conductivity values K_m of sulphuric acid (considered as the measure of apparent conductivity of the interaction between the electrolyte and the foam) of all the MFAB cells are above that of the non-porous dense material. From Figure 4, the curve of the Sb-Pb dense cell was between [670-690] (µs/cm) and all the curves of ESR foams cells were between [705-760] (µs/cm). This clearly shows the superior electrochemical performance of all the foams compared to the use of the dense alloy (non-porous) of the same composition as the matrix of foam electrodes, regardless of their porosity or cell diameter. This is due to the remarkable specific active surface area of these foam anodes [50], which means in another word that when the anode is cellular, its interactions with the electrolyte are important because of the large surface where redox reactions occur leading to an important EEC.

When the electrode was immersed in the electrolyte (the beginning of the curves in Figure 4), spontaneous and automatic discharge without charge/discharge of the cells begun, then continued slowly, until the equilibrium of the electron flowing in the circuit was reached; which means that the electrical conductivity has reached the lower limit or a final threshold. There was a clear demarcation

in the representative curve of SbSPb20 due to an unexpected change in the temperature of the electrolyte during the measurement.

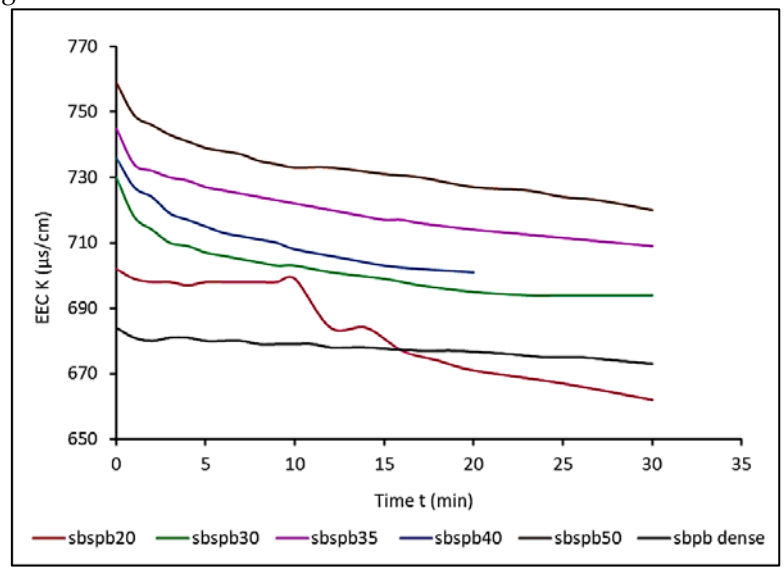

Figure 4. Curves comparing the electrical conductivity EEC of sulphuric acid from all cells with the dense SbPb electrode.

Milusheva stated that the concentration of the acid electrolyte in a Pb-air cell varies with the state of charge in a similar way to a conventional lead acid battery [30] according to this scheme of reactions:

Reaction at cathode:

$$O_2 + 2H_2SO_4 + 4e^- \rightarrow 2H_2O + 2SO_4{}^{-2} \quad (1)$$

Reaction at anode:

$$Pb + 2SO_4{}^{-2} \rightarrow 2PbSO_4 + 4e^- \quad (2)$$

The overall reaction:

$$O_2 + Pb + 2H_2SO_4 \leftrightarrow PbSO_4 + 2H_2O \quad (3)$$

Hassein-Bey et al. [42] noticed that the cells of these foams were coated with lead oxides and lead carbonates as shown in Figure 5, after energy dispersive X-ray spectroscopy (EDXS) performed with JOEL JSM-6360. The two types of crystals (marked by blue and red cross) were composed of Pb and O and (perhaps undetectable H), but there was no Sb suggesting that no antimony oxides resulted during the ESR process because of the processing temperature close to that of antimony melting temperature.

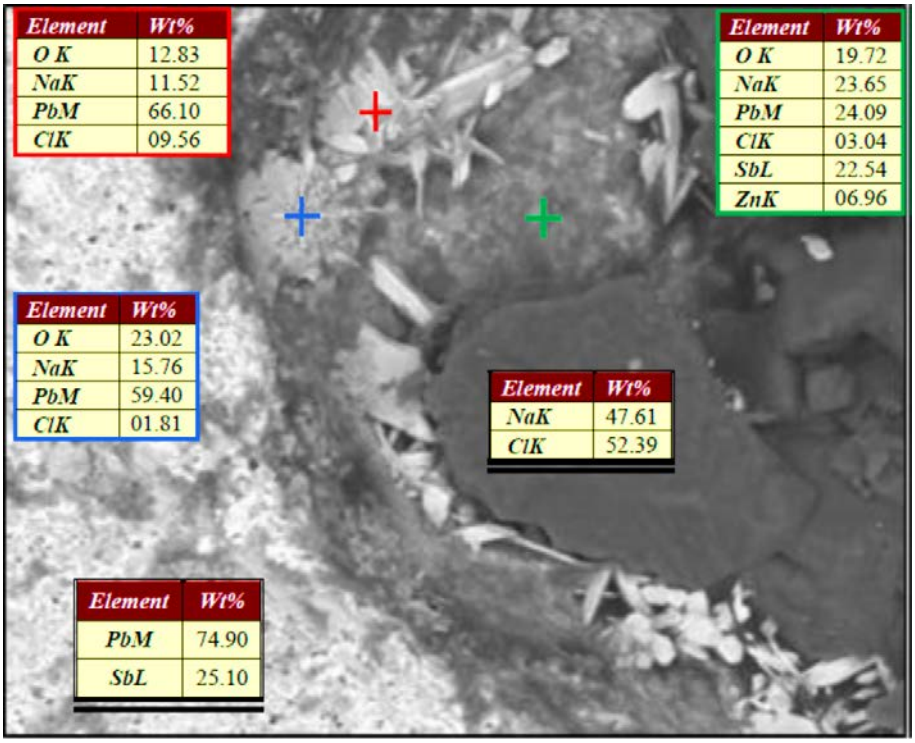

Figure 5. Magnification of the film existing between salt grain and antimonial lead alloy matrix in SbS40 ESR foam sample obtained with JOEL JSM-6360 before NaCl leahing. The chemical composition of the different species present was revealed with EDXS.

Figure 6 confirms that after salt leaching, only lead oxides and lead carbonates exist according to the EDXS of the inner cell wall.

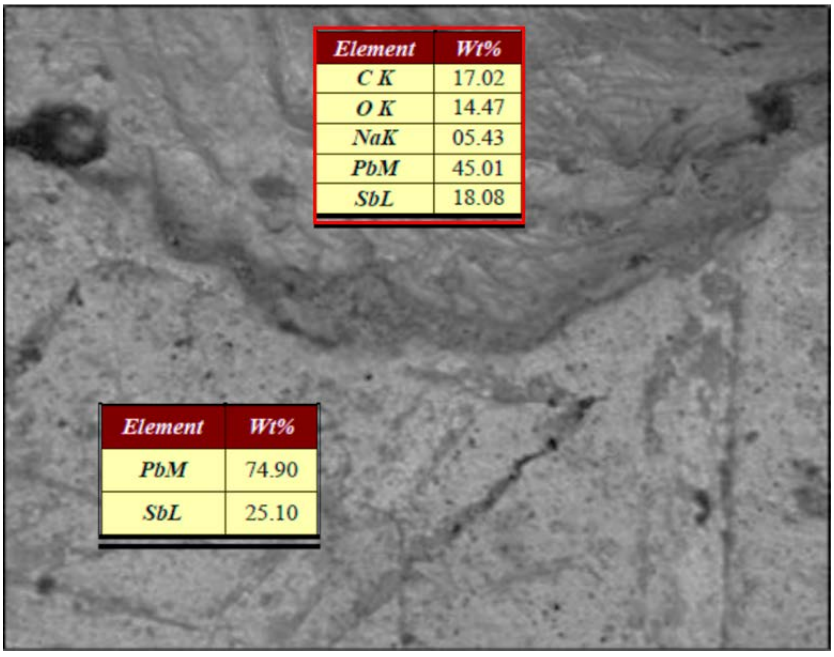

Figure 6. EDXS of SbS40 revealing the chemical composition of cell matrix and inner cell wall after salt leaching.

Mai et al.[51] investigated nano structured PbO2-PANi composites for electrocatalytic oxidation of methanol in sulphuric acid medium and confirmed that lead dioxide is known to be a material

 doi:10.20944/preprints202305.0296.v1

with excellent chemical stability, high conductivity and chemical inertia for electrolysis in acid medium. So, when the current is delivered, it is believed that these coating elements (obviously lead carbonates) were oxidised at the anode, allowing O_2 from the air to be reduced at the cathodes and suggesting that the Pb dense electrode didn't react. This reaction scheme is suggested:

At the anode, the oxidation is undertaken by the CO_2/CO_3^{2-} couple giving the following anodic half-cell reaction (equation 4):

$$PbCO_3 + H_2SO_4 \rightarrow CO_2 + PbSO_4 + H_2O + 2e^- \quad (4)$$

At the cathode, the reduction is undertaken by the O_2/H_2O couple giving the following cathodic half-cell reaction (equation 5):

$$O_2 + 2H_2SO_4 + 4e^- \rightarrow 2H_2O + 2SO_4{}^{-2} \quad (5)$$

Two claims need verification: the first one is the non-chemical reactivity of the Pb dense electrode by the weighing method when ESR electrodes were used; and the second one is the chemical reactivity of the Pb dense electrode when no ESR foam electrodes were used, using FTIR spectroscopy of the external surface of SbPb dense sample before and after MAB cell tests.

3.4. Identification of electrodes chemical reactivity

In order to identify which electrode did contribute to the electrochemical reactions and therefore delivered the cells current, it was necessary to weigh the electrodes before (m_0) and after (m_f) each test. Then, the difference in mass $\Delta mD=mD_0-mD_f$ (in g) of the Pb dense lead electrode and $\Delta mF=mF_0-mF_f$ (in g) of the 25% Sb-Pb ESR foam electrode calculated from these weighed masses were plotted for each ESR foam diameter, as shown in Figure 7. The SbPb dense material (non-porous) was considered too. If this difference is positive, it means that a loss of mass has occurred at the electrode after test.

It seems that the Pb dense electrode did not react because its difference in mass ΔmD is constant (0.001 g) for the SbSPb20, SbSPb30, SbSPb35 and SbSPb40. While ΔmF of these foams is positive and changes significantly. This means that these four tested ESR anodes have lost some of their mass proportion after running their MFAB cells except for the SbSPb 50 (the balance was changed). While the SbPb dense electrodes confirmed our claim that in the absence of the open cells of the foams (when the electrode is not porous), this cell inverts and it is the lead electrode (which was inert in the presence of the ESR foams electrodes) that reacts according to the pattern expressed by the reactions (1),(2),(3).

It looks like these cells are selective: the electrical current is produced from the reactions of the lead carbonates coating the inner surface of the open cells of the ESR foams when they are used. In the absence of these open cell foams produced by the ESR process, the electrode made of the same alloy as the cell matrix does not react, thus turning the cell into a lead-air battery. It is therefore preferable to use cellular antimonial lead electrodes rather than antimonial lead electrodes in MAB cells.

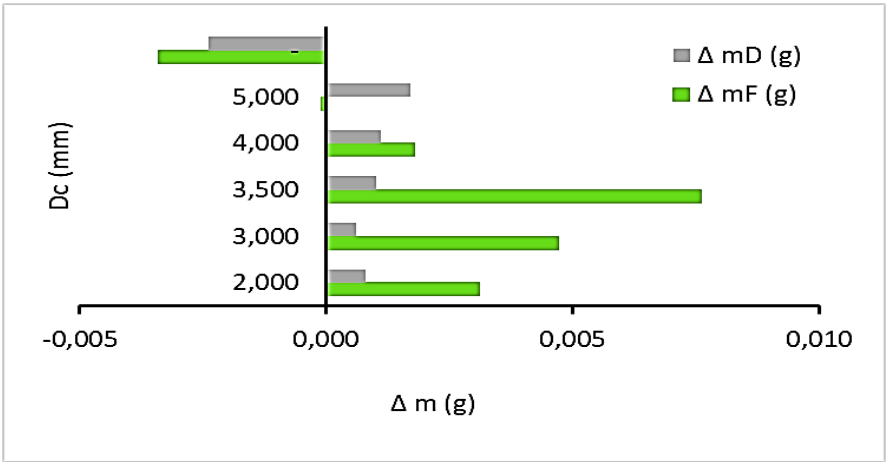

Figure 7. Analysis of the difference in mass ΔmD of the Pb dense lead electrode and ΔmF of the 25% SbPb ESR foam electrode

3.5. FTIR of SbPb dense electrode

In order to confirm the chemical reactivity of the ESR foams electrodes when present in battery cell and then the reactivity of pure Pb dense electrode in their absence, the Fourier-transform infrared spectroscopy (FTIR) analysis of the external surface of the SbPb dense sample was performed, before and after MFAB cell test. This analysis was carried out by using SHIMADZU FTIR–8400 in the range of 4000–400 cm^{-1}. Figure 8 shows the spectra where the significant peaks before MFAB cell test, were found in the regions 1600–1400 cm^{-1} and 1200–1100 cm^{-1}. They are two broader peaks at wavelength 1419 cm^{-1} due to the S=O stretching caused by the sulphate group and at 1091cm^{-1} due to the hydrogénosulfate (HSO_4). This revealed the contribution of Pb dense electrode to the electrochemical reaction by detecting the presence of HSO_4- and $PbSO_4$ like in lead-air batteries. After MFAB cell test, The small peak at wavelength 683 cm^{-1} and the peaks at the 410 cm^{-1} are due to the result of lead sulphate $PbSO_4$ vibration. This $PbSO_4$ deposited on SbPb dense electrodes (causing their chemical inertia) after Pb electrode oxidation as an anode. Similarly, another intense and tight peak was found at 2345 cm^{-1} which is characteristic of CO_2. It is the result of some lead carbonate decomposition (from the SbPb dense electrode) to $PbSO_4$ in presence of H_2SO_4. This is confirmed earlier by its ΔmF and ΔmD of the SbPb dense cell test.

In spite of all these data, it is difficult to specify exactly the electrode reactions occurring during the MFAB cells running.

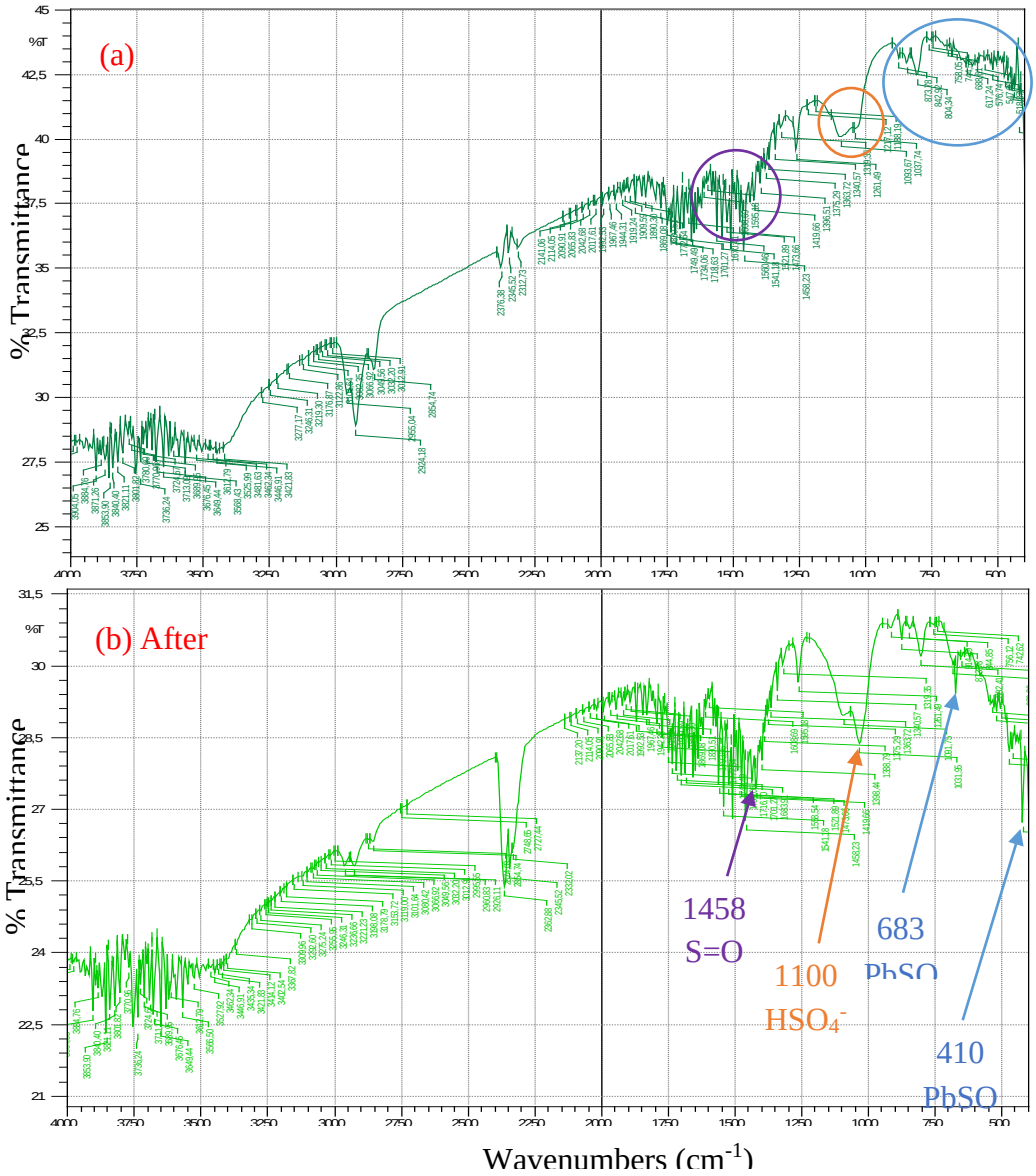

Figure 8. FTIR spectra of SbPb dense electrode (a) before and (b) after MFAB

3.6. Effect of cell diameter of ESR foam anode on the measured effective electrical conductivity

In the replication process, the morphology and pore size are very similar to those of the NaCl particles used. It has already been reported for this type of foam that pore size affects the conductivity of the foam [52]. As stated in this reference, for a fixed porosity, a smaller pore size leads to a lower electrical conductivity, as more air is trapped between the matrix and the NaCl particles, due to the larger interfacial area. A larger pore size leads to a better bonding structure, which results in a higher electrical conductivity, which is in our case effectively represented in Figure 9.

 doi:10.20944/preprints202305.0296.v1

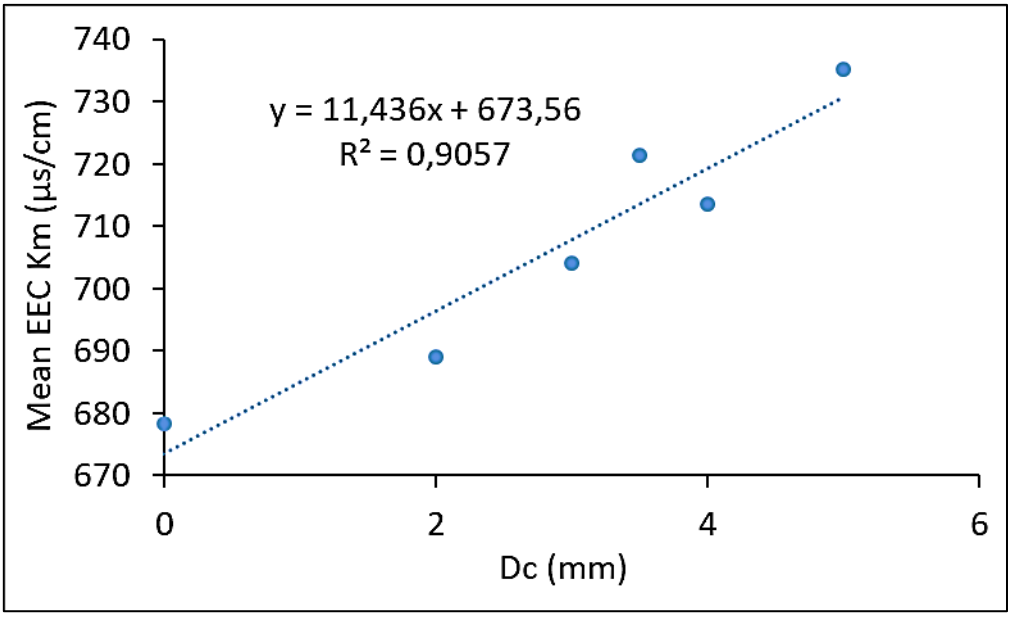

Figure 9. Linear relationship between effective electrical conductivity and cell diameter of MFAB

It is clear that a linear relationship exists between the EEC and the cell diameter D_c and that ESR foams performed better than the same non-porous dense alloy as in equation (4):

$$K_m = 11.44D_c + 673.56 \quad (4)$$

This empirical relationship allows an overall prediction of effective electrical conductivity of future 25 % antimony-lead alloy foams produced with this ESR process for a specific cell diameter before the elaboration of MFAB cells.

4. Conclusion

Metal-air batteries, powered by metal oxidation and oxygen reduction, have been intensely focused upon as promising next-generation high-energy batteries. In this innovative research on metal air battery cells, 25% SbPb open cell foams, with a cell diameter of between 2mm and 5mm, have been successfully proposed as an electrode and have performed much better than the same non-porous electrode made of the same dense alloy. The large accessible surface area of these open cell metal foams, makes them attractive as electrodes for battery cells, which can lighten them, too. The oxidation of lead carbonates coating the internal cells and resulting during the ESR process, are believed to be the source of the electrical current of these primary cells.

An empirical relation was proposed to predict the effective electrical conductivity of such foams in terms of cell diameter in Lead-air battery cells.

Research is continuing with the aim of producing a final prototype which will be developed and characterised soon. Further improvement of this system could lead to its potential use in the automotive industry.

References

1. Hossain, M.D.; Islam, M.M.; Hossain, M.J.; Yasmin, S.; Shingho, S.R.; Ananna, N.A.; Mustafa, C.M. Effects of additives on the morphology and stability of PbO2 films electrodeposited on nickel substrate for light weight lead-acid battery application. *Journal of Energy Storage* **2020**, *27*, 101108, doi:https://doi.org/10.1016/j.est.2019.101108.
2. Kaneko, K.; Hori, K.; Noda, S. Nanotubes make battery lighter and safer. *Carbon* **2020**, *167*, 596-600, doi:https://doi.org/10.1016/j.carbon.2020.06.042.

3. Wu, F.; Maier, J.; Yu, Y. Guidelines and trends for next-generation rechargeable lithium and lithium-ion batteries. *Chemical Society Reviews* **2020**, *49*, 1569-1614.
4. Dunlop, J.; Beauchamp, R. Making space nickel/hydrogen batteries lighter and less expensive. *NASA STI/Recon Technical Report N* **1987**, *88*, 13530.
5. Shaffer, B.; Auffhammer, M.; Samaras, C. Make electric vehicles lighter to maximize climate and safety benefits. **2021**.
6. Nyholm, L. Lighter and safer. *Nature Energy* **2020**, *5*, 739-740.
7. Landi, B.J.; Ganter, M.J.; Cress, C.D.; DiLeo, R.A.; Raffaelle, R.P. Carbon nanotubes for lithium ion batteries. *Energy & Environmental Science* **2009**, *2*, 638-654.
8. Clemente, A.; Costa-Castelló, R. Redox flow batteries: A literature review oriented to automatic control. *Energies* **2020**, *13*, 4514.
9. Linden, D.; Reddy, T. Lead acid batteries. *Handbook of batteries* **2002**, 1-88.
10. Logeshkumar, S.; Manoharan, R. Influence of some nanostructured materials additives on the performance of lead acid battery negative electrodes. *Electrochimica Acta* **2014**, *144*, 147-153.
11. Hao, H.; Chen, K.; Liu, H.; Wang, H.; Liu, J.; Yang, K.; Yan, H. A review of the positive electrode additives in lead-acid batteries. *Int. J. Electrochem. Sci* **2018**, *13*, 2329-2340.
12. Pletcher, D.; Wills, R. A novel flow battery—A lead acid battery based on an electrolyte with soluble lead (II): III. The influence of conditions on battery performance. *Journal of Power Sources* **2005**, *149*, 96-102.
13. Jullian, E.; Albert, L.; Caillerie, J. New lead alloys for high-performance lead–acid batteries. *Journal of power sources* **2003**, *116*, 185-192.
14. Osório, W.R.; Rosa, D.M.; Garcia, A. The roles of cellular and dendritic microstructural morphologies on the corrosion resistance of Pb–Sb alloys for lead acid battery grids. *Journal of power sources* **2008**, *175*, 595-603.
15. Li, A.; Cheni, Y.; Chen, H.; Shu, D.; Li, W.; Wang, H.; Dou, C.; Zhang, W.; Chen, S. Electrochemical behavior and application of lead–lanthanum alloys for positive grids of lead-acid batteries. *Journal of power sources* **2009**, *189*, 1204-1211.
16. Abdelghani-Idrissi, S. La charge rapide d'une batterie métal-air par la maîtrise de la fluidique diphasique. Université Paris sciences et lettres, 2020.
17. Hariprakash, B.; Mane, A.; Martha, S.; Gaffoor, S.; Shivashankar, S.; Shukla, A. A low-cost, high energy-density lead/acid battery. *Electrochemical and Solid-State Letters* **2004**, *7*, A66.
18. Tabaatabaai, S.; Rahmanifar, M.; Mousavi, S.; Shekofteh, S.; Khonsari, J.; Oweisi, A.; Hejabi, M.; Tabrizi, H.; Shirzadi, S.; Cheraghi, B. Lead-acid batteries with foam grids. *Journal of power sources* **2006**, *158*, 879-884.
19. Bullock, K.R. Lead/acid batteries. *Journal of power sources* **1994**, *51*, 1-17.
20. Martha, S.; Hariprakash, B.; Gaffoor, S.; Trivedi, D.; Shukla, A. A low-cost lead-acid battery with high specific-energy. *Journal of Chemical Sciences* **2006**, *118*, 93-98.
21. Albert, L.; Chabrol, A.; Torcheux, L.; Steyer, P.; Hilger, J. Improved lead alloys for lead/acid positive grids in electric-vehicle applications. *Journal of power sources* **1997**, *67*, 257-265.
22. Hariprakash, B.; Gaffoor, S. Lead-acid cells with lightweight, corrosion-protected, flexible-graphite grids. *Journal of power sources* **2007**, *173*, 565-569.
23. LaFollette, R.M. Design and performance of high specific power, pulsed discharge, bipolar lead acid batteries. In Proceedings of the Proceedings of the Tenth Annual Battery Conference on Applications and Advances, 1995; pp. 43-47.
24. Lach, J.; Wróbel, K.; Wróbel, J.; Podsadni, P.; Czerwiński, A. Applications of carbon in lead-acid batteries: a review. *Journal of Solid State Electrochemistry* **2019**, *23*, 693-705.

25. Liu, Q.; Pan, Z.; Wang, E.; An, L.; Sun, G. Aqueous metal-air batteries: Fundamentals and applications. *Energy Storage Materials* **2020**, *27*, 478-505.
26. Olabi, A.G.; Sayed, E.T.; Wilberforce, T.; Jamal, A.; Alami, A.H.; Elsaid, K.; Rahman, S.M.A.; Shah, S.K.; Abdelkareem, M.A. Metal-air batteries—a review. *Energies* **2021**, *14*, 7373.
27. Das, S.K.; Lau, S.; Archer, L.A. Sodium–oxygen batteries: a new class of metal–air batteries. *Journal of Materials Chemistry A* **2014**, *2*, 12623-12629.
28. Rahman, M.A.; Wang, X.; Wen, C. High energy density metal-air batteries: a review. *Journal of The Electrochemical Society* **2013**, *160*, A1759.
29. Han, X.; Li, X.; White, J.; Zhong, C.; Deng, Y.; Hu, W.; Ma, T. Metal–air batteries: from static to flow system. *Advanced Energy Materials* **2018**, *8*, 1801396.
30. Milusheva, Y.; Popov, I.; Shirov, B.; Banov, K.; Boukoureshtlieva, R.; Obretenov, W.; Naidenov, V. Lead-Air Electrochemical System with Acid Electrolyte. *Journal of The Electrochemical Society* **2021**, *168*, 060524, doi:10.1149/1945-7111/ac0862.
31. Olabi, A.G.; Sayed, E.T.; Wilberforce, T.; Jamal, A.; Alami, A.H.; Elsaid, K.; Rahman, S.M.A.; Shah, S.K.; Abdelkareem, M.A.J.E. Metal-air batteries—a review. **2021**, *14*, 7373.
32. Pei, P.; Wang, K.; Ma, Z. Technologies for extending zinc–air battery's cyclelife: A review. *Applied Energy* **2014**, *128*, 315-324, doi:https://doi.org/10.1016/j.apenergy.2014.04.095.
33. Akhtar, N.; Akhtar, W.J.I.J.o.E.R. Prospects, challenges, and latest developments in lithium–air batteries. **2015**, *39*, 303-316.
34. Chang, S.; Hou, M.; Xu, B.; Liang, F.; Qiu, X.; Yao, Y.; Qu, T.; Ma, W.; Yang, B.; Dai, Y.J.A.F.M. High-performance quasi-solid-state Na-air battery via gel cathode by confining moisture. **2021**, *31*, 2011151.
35. Farsak, M.; Kardaş, G. 2.12 Electrolytic Materials. **2018**.
36. Zhao, Y.; Huang, G.; Zhang, C.; Peng, C.; Pan, F. Effect of phosphate and vanadate as electrolyte additives on the performance of Mg-air batteries. *Materials Chemistry and Physics* **2018**, *218*, 256-261, doi:https://doi.org/10.1016/j.matchemphys.2018.07.037.
37. Sumathi, S.; Sethuprakash, V.; Basirun, W.; Zainol, I.; Sookhakian, M.J.J.o.s.-g.s.; technology. Polyacrylamide-methanesulfonic acid gel polymer electrolytes for tin-air battery. **2014**, *69*, 480-487.
38. Ashby, M.F.; Evans, T.; Fleck, N.; Hutchinson, J.W.; Wadley, H.N.G.; Gibson, L.J. *Metal Foams: A Design Guide*; Elsevier Science: 2000.
39. Song, M.J.; Kim, I.T.; Kim, Y.B.; Shin, M.W. Self-standing, binder-free electrospun Co3O4/carbon nanofiber composites for non-aqueous Li-air batteries. *Electrochimica Acta* **2015**, *182*, 289-296.
40. Zhu, G.; Li, X.; Liu, Y.; Mao, Y.; Liang, Z.; Ji, Z.; Shen, X.; Sun, J.; Cheng, X.; Mao, J. Scalable surface engineering of commercial metal foams for defect-rich hydroxides towards improved oxygen evolution. *Journal of Materials Chemistry A* **2020**, *8*, 12603-12612.
41. Wang, H.-F.; Xu, Q. Materials Design for Rechargeable Metal-Air Batteries. *Matter* **2019**, *1*, 565-595, doi:https://doi.org/10.1016/j.matt.2019.05.008.
42. Hassein-Bey, A.H.; Belhadj, A.-E.; Gavrus, A.; Abudura, S. Elaboration and Mechanical-Electrochemical Characterisation of Open Cell Antimonial-lead Foams Made by the "Excess Salt Replication Method" for Eventual Applications in Lead-acid Batteries Manufacturing. *Kemija u industriji: Časopis kemičara i kemijskih inženjera Hrvatske* **2020**, *69*, 387-398.
43. Prengaman, R.D. SECONDARY BATTERIES – LEAD– ACID SYSTEMS | Lead Alloys. In *Encyclopedia of Electrochemical Power Sources*, Garche, J., Ed.; Elsevier: Amsterdam, 2009; pp. 648-654.

44. Hill, R.J. Structure of PbSb2O6 and its relationship to the crystal chemistry of PbO2 in antimonial lead-acid batteries. *Journal of Solid State Chemistry* **1987**, *71*, 12-18, doi:https://doi.org/10.1016/0022-4596(87)90136-8.
45. Dharmasena, K.; Wadley, H. Electrical conductivity of open-cell metal foams. *Journal of materials research* **2002**, *17*, 625-631.
46. Ashby, M.F.; Evans, A.G.; Fleck, N.A.; Gibson, L.J.; Hutchinson, J.W.; Wadley, H.N.G. *Metal Foams: A Design Guide*; Butterworth-Heinemann: 2000; p. 263.
47. Liu, P.; Li, T.; Fu, C. Relationship between electrical resistivity and porosity for porous metals. *Materials Science and Engineering: A* **1999**, *268*, 208-215.
48. Majima, H.; Peters, E.; Awakura, Y.; Park, S.K. Electrical conductivity of acidic sulfate solution. *Metallurgical Transactions B* **1987**, *18*, 41-47, doi:DOI: https://doi.org/10.1007/BF02658430.
49. Biagetti, R. Fabrication of lead-acid batteries. **1973**.
50. Newman, J.; Tiedemann, W. Porous-electrode theory with battery applications. *AIChE Journal* **1975**, *21*, 25-41.
51. Mai, T.T.T.; Phan, T.B.; Pham, T.T.; Vu, H.H. Nanostructured PbO2-PANi composite materials for electrocatalytic oxidation of methanol in acidic sulfuric medium. *Advances in Natural Sciences: Nanoscience and Nanotechnology* **2014**, *5*, 025004.
52. Ma, X.; Peyton, A.; Zhao, Y. Measurement of the electrical conductivity of open-celled aluminium foam using non-contact eddy current techniques. *NDT & E International* **2005**, *38*, 359-367.